Lasers in Surgery and Medicine 26:405–414 (2000)

A Study of Aminolevulinic Acid–Induced Protoporphyrin IX Fluorescence Kinetics in the Canine Oral Cavity

Vijay V. Vaidyanathan, PhD,[1] Sohi Rastegar, PhD,[1]* Theresa W. Fossum, DVM, PhD,[2] Patricia Flores,[2] Egbertus W. van der Breggen, MS,[3] Norman G. Egger, MD,[3] Steven L. Jacques, PhD,[4] and Massoud Motamedi, PhD[4]

[1]Bioengineering Program, Texas A&M University, College Station, Texas 77843
[2]School of Veterinary Medicine, Texas A&M University, College Station, Texas 77843
[3]University of Texas Medical Branch at Galveston, Texas 77555
[4]Oregon Medical Laser Center, Portland, Oregon 97225

Background and Objective: **5-Aminolevulinic acid–induced protoporphyrin IX is a promising photosensitizer that could enhance the spectroscopic contrast between normal and diseased oral tissues. Knowledge of the pharmacokinetics and effects on tissue type are important for diagnostic and therapeutic procedures.**
Study Design/Materials and Methods: **Dogs randomly were administered five doses of 5-aminolevulinic acid: 5, 25, 50, 75, and 100 mg/kg. The fluorescence was recorded from buccal mucosa, gums, tongue, and facial skin using a fiberoptic probe connected to an optical multichannel analyzer. Blood samples were collected for hematologic and serum biochemical analysis. Pharmacokinetic parameters of interest were estimated using a compartmental model.**
Results: **Protoporphyrin fluorescence at all sites reached a peak in 2–6 hours, and returned to baseline in 24–31 hours, depending on the dose. Plasma protoporphyrin peaked earlier than oral tissues.**
Conclusion: **The rate of synthesis of protoporphyrin, and its conversion to heme products are dose dependent. Different tissues have different pharmacokinetic response. Lasers Surg. Med. 26:405–414, 2000.**

Key words: in vivo; pharmacokinetics; dosage; oral tissue

INTRODUCTION

Fluorescence spectroscopic detection (FSD) and photodynamic therapy (PDT) may provide an effective approach for early detection and treatment of oral cancer. Autofluorescence, the natural fluorescence of tissue, has been used to distinguish between normal and neoplastic tissue. However, the differentiation is largely dependent on the biochemical composition and histomorphologic structure of the tissues that undergo a change during transformation from normal to malignant. Ingrams et al. [1] investigated the use of autofluorescence spectra at excitation wavelengths of 370 and 410 nm to distinguish between normal oral mucosa and abnormal tissue samples and found more prominent differences at 410 nm. Yang et al. [2] examined the ultraviolet excitation spectrum in the range of 275–450 nm for malignant and benign breast tissues and attributed the differences observed to an alteration in specific proteins.

Photosensitizers that are more selectively retained in neoplastic tissues could enhance the reliability of optical diagnosis and photodynamic therapy. Fluorescent dyes such as photofrin have

Contract grant sponsor: Department of Energy Center for Excellence for Medical Laser Applications; Contract grant number: DOE-FG03-95ER61971.

*Correspondence to: Sohi Rastegar, Bioengineering Program, Texas A&M University, College Station, TX 77843.

Accepted 24 September 1999

been used in studies on photodynamic therapy. Hayata and Kato [3] reported success with photodynamic therapy in bronchial tumors using photofrin. Recently, Kelley et al. [4] reported increased efficacy of in vitro photofrin photosensitization of human oral squamous cell carcinoma by adding iron and ascorbate. Fan et al. [5] demonstrated good healing after the use of meta tetrahydroxyphenyl chlorin (mTHPC) as a new photosensitizer in PDT of malignant disease of the oral cavity. Photosensitizers like photofrin have been widely used in photodynamic therapy and tissue differentiation; however, adverse side effects such as prolonged cutaneous photosensitization have limited their use. Orenstein et al. [6] reported a higher porphyrin accumulation and PDT selectivity in the colon carcinoma model due to 5-aminolevulinic acid (ALA) –induced protoporphyrin IX (PpIX) than photofrin.

ALA is a naturally occurring precursor of heme. The native compound is not a photosensitizer, but in certain types of cells and tissues, it is metabolized to the photosensitizer PpIX in the body [7]. Intracellular porphyrin localization and photoactivation have been reported to occur first within the plasma membrane. After several hours of incubation, redistribution within the cell occurs to include the nuclear membrane and other organelles such as mitochondria and lysosomes [8,9]. When excited with suitable wavelength of light (~410 nm), PpIX emits characteristic fluorescence in the red spectrum (636 nm). In a recent in vitro study, Wilson et al. [10] investigated the subcellular mitochondrial localization of the photodynamic sensitizers photofrin and ALA-induced PpIX in radiation-induced fibrosarcoma (RIF) tumor cells. As with photofrin, ALA-induced PpIX showed weaker localization in the mitochondria in RIF-8A than in RIF-1 cells.

In an investigation that used a hamster cheek-pouch model, van der Breggen et al. [11] reported a significant increase in tissue autofluorescence and ALA-induced PpIX fluorescence during transformation of buccal mucosa from normal to premalignant to malignant. The fluorescence measurements were found to correlate well with histopathologic assessment of tumor development. Abels et al. [12] investigated in vivo kinetics and spectra of ALA-induced PpIX fluorescence in amelanotic melanoma of hamsters for three doses of ALA: 100, 500, and 1,000 mg/kg. The transient selectivity of PpIX in tumors was attributed to an earlier and higher uptake of ALA in the neoplastic tissue, most likely as a result of increased vascular permeability of tumors or reduced activity of the enzyme ferrochelatase in tumors.

The first clinical report of the use of orally administered ALA as a photosensitizing agent to induce photodynamic tumor necrosis was presented by Grant et al. [13]. The study showed that oral squamous cell carcinomas can synthesize and accumulate photosensitizing levels of PpIX after oral ALA administration. In recent studies, Leunig et al. [14] were able to detect PpIX fluorescence in the oral mucosa of 16 patients after topical application of ALA. PpIX in neoplastic tissue was found to accumulate earlier than in nonneoplastic tissue with maximum fluorescence contrast seen 1–2 hours after application [14]. Fan et al. [15] investigated the efficacy of photodynamic therapy by using ALA for premalignant and malignant lesions of the oral cavity after oral administration of a dose of 60 mg/kg and treatment with laser light at 628 nm (100 J/cm^2). The depth of necrosis was found to vary from 0.1 to 0.3 mm, but complete epithelial necrosis was found to be present in all cases. Recently, Webber et al. [16] reported abnormal liver functions and photosensitization in patients given 30 or 60 mg/kg of ALA preoperatively (before abdominal surgery).

ALA-induced PpIX is a promising photosensitizer that could be used in noninvasive diagnosis and photodynamic therapy of oral cancers. Because the oral cavity is easily accessible with flexible optical fibers, it is a suitable site for fluorescence detection. Our study has particular relevance to the use of ALA for diagnosis and therapy of oral cancers in veterinary medicine. The aim is to investigate the effect of dosage and tissue type on ALA-induced fluorescence kinetics. Because anesthesia may affect the animal's metabolism and, thus, the production of PpIX at the site of interest, awake dogs were studied. Although there have been fluorescence studies conducted with ALA on small animals such as hamsters, there are few studies reported on larger animals. Before use in humans, clear understanding of the effect of dosage and tissue type on ALA-induced fluorescence is needed. Dogs, like humans, are known to develop oral cancer naturally, and their oral cavity is similar to that of humans. Thus, dogs are a good model in which to study the pharmacokinetics of ALA.

MATERIALS AND METHODS

Five female dogs, aged 2–4 years with an average weight of 22 kg, were used in the study.

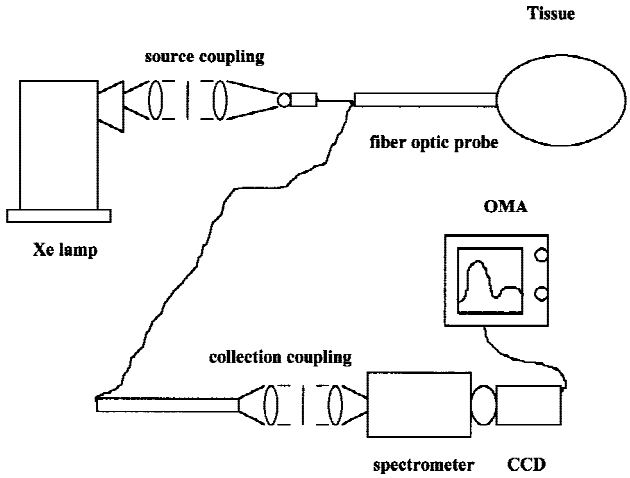

Fig. 1. Experimental set-up for fluorescence measurement from the oral cavity and skin of normal dogs. The light source was a 150 W xenon lamp, filtered to provide ultraviolet light for excitation (400 ± 30 nm, Melles Griot type 03FIB002). The fluorescence light was collected by another fiber and guided to a spectrometer, interfaced with an optical multichannel analyzer (OMA). CCD, charge-coupled device.

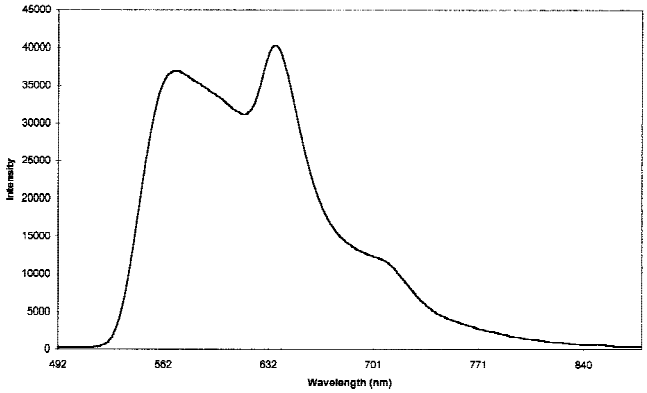

Fig. 2. Typical fluorescence spectrum obtained from the oral cavity (gingiva) of a dog. The second sharper peak corresponds to characteristic protoporphyrin IX (PpIX) fluorescence. The fluorescence data were recorded as ratio of intensity at 636 nm:intensity at 594 nm. ALA, aminolevulinic acid.

Three sites in the oral cavity (buccal mucosa, tongue, and gums) were used for fluorescence detection. In addition, fluorescence was also measured from the facial skin of the dogs. The hair from the area of measurement was shaved with an electric razor before measurement. Tissue autofluorescence was measured from the four sites of interest, before administration of ALA. A bifurcated fiber optic probe was used to deliver excitation and collect the emitted fluorescence (636 nm). The light source was a 150 W xenon lamp, filtered to provide ultraviolet light for excitation (400 ± 30 nm, Melles Griot type 03FIB002). The fluorescence light was collected by another fiber and guided to a spectrometer, interfaced with an optical multichannel analyzer (OMA). The set-up is shown in Figure 1. The fluorescence measurements were made in a darkened laboratory with the probe contacting the site at a perpendicular angle. The probe was cleaned after measurement at each site.

The animals were fasted overnight. Before the procedure, restives were sedated by intramuscular injection of acepromazine (2 mg) and a catheter was inserted into the cephalic vein. 5-ALA (Sigma Chemical Company, St. Louis, MO, purity 98%) was dissolved in sterile phosphate buffered saline at a concentration of 80 mg/ml and immediately administered through the cephalic catheter over 5 minutes. The ALA-induced fluorescence was measured from the sites previously evaluated for autofluorescence. All the fluorescence data was recorded as a ratio of intensities observed at 636 nm (R-red) and 595 nm (O-orange), i.e., R/O. Figure 2 shows typical fluorescence spectrum obtained from the gums of a dog 2 hours after ALA administration. The red wavelength band is significant because of the characteristic PpIX fluorescence peak in the red spectrum, whereas the orange wavelength was chosen to minimize the effect of tissue optics on measurements [11,17]. Five doses of ALA, i.e., 5, 25, 50, 75, and 100 mg/kg, were administered intravenously to the animals. Two dogs received three different doses and three dogs received four different doses. A "wash-out" period of 1 week between doses ensured that residual PpIX was not present when the subsequent dose was administered. Fluorescence data were collected from the target areas at 1, 2, 3, 4, 6, 7, 24, 27, and 31 hours, respectively, after administration of ALA. At each site, five measurements were taken and their values averaged. The animals were housed in a darkened kennel for 24 hours after treatment to prevent cutaneous phototoxicity.

Because two dogs received doses of 100 mg/kg, indwelling catheters were inserted for 24 hours to evaluate the presence of protein, blood, or both, in the urine. Total urinary porphyrins were determined by using the technique described by Schwartz et al. [18,19]. Total porphyrin concentration in plasma was determined by extracting 2-μl plasma samples with 0.3 ml of ethyl acetate-glacial acetic acid (2:1 by volume) and 0.3 ml of 0.5 N HCl, and measuring porphyrins by spectrophotometry (excitation wavelength 400 nm, emission wavelength 650 nm) [19].

TABLE 1. Analysis of Variance for Autofluorescence and 5-Aminolevulinic Acid–Induced Fluorescence Ratios*

Hour	Source	Degrees of freedom	Type III SAS	Mean square	F value	PR > F
0	A*B (Interaction)	9	0.1678	0.01864	1.91	0.0750
1	A*B (Interaction)	12	25.708	2.143	3.19	0.0030
24	A*B (Interaction)	12	1.245	0.104	1.38	0.2260

*Hour 0 = autofluorescence. Decision: If α (0.05) < pr value for A*B, accept null hypothesis, otherwise reject null hypothesis for alternate hypothesis. Null hypothesis for hour 0: Effect of sites (B) on autofluorescence is same for all weeks (A) of measurement. Alternate hypothesis for hour 0: Effect of sites (B) on autofluorescence is not the same for all weeks (A) of measurement. Null hypothesis for hour 1 and 24: Effect of sites (B) on fluorescence is same for all doses (A). Alternate hypothesis for hour 1 and 24: Effect of sites (B) on fluorescence is not the same for all doses (A).

Statistical analysis of the fluorescence (R/O) data determined interaction between sites and doses of ALA administered. The hypotheses were as follows: null hypothesis, no interaction between dose and site; alternate hypothesis, interaction present between dose and site. The fluorescence data were arranged in the form of a split-plot design, with two factors: factor A was the ALA dose, and factor B was the site of fluorescence measurement. Analysis of variance (ANOVA) in the fluorescence data were done by using SAS (Statistical Analysis Systems) code.

Mathematical modeling techniques provide convenient and useful descriptions of metabolic processes to be formulated. Mathematical models are used to estimate internal (inaccessible) parameters of physiological interest [20]. Abels et al. [12] developed a three-compartment model to simulate fluorescence kinetics in tumors. It was assumed that ALA/PpIX are metabolized/eliminated after first-order processes. In their model, as in this study, the measured fluorescence from tissue was assumed to be proportional to the amount of PpIX in tissue. Their model incorporated the losses of ALA to urine and other tissues before reaching target cells. Their equation for the accumulation of PpIX as a function of time is:

$$P(t) = \frac{M_0}{k_1}\frac{k_0}{k_x}\left[\frac{\exp(-k_x t) - \exp(-k_2 t)}{k_2 - k_x} + \frac{\exp(-k_2 t) - \exp(-k_1 t)}{k_2 - k_1}\right] \quad (1)$$

where M_0 is the initial serum concentration of ALA, k_0 is the uptake by the target tissue of interest, k_1 is the rate of PpIX synthesis, k_2 is the conversion of PpIX to heme products, and k_x is the rate of ALA removal from the serum by urine losses and uptake by other tissues. An SAS code was written by using least-squares and Marquardt method to estimate the rate of PpIX synthesis and the conversion of PpIX to heme products, by fitting the fluorescence data to the governing equation of the compartmental model (Eq. 1).

RESULTS

The dogs were stable throughout the duration of the study, except for vomiting noted at doses greater than 5 mg/kg. None of the dogs vomited when administered 5 mg/kg of ALA. The frequency of vomiting was higher for higher doses. For the 25 mg/kg dose: two of four dogs vomited once, one dog (in heat) vomited twice, whereas one did not vomit at all. One of the dogs that received higher doses (>25 mg/kg) did not vomit at all. For the dose of 50 mg/kg: two dogs vomited twice, whereas one dog vomited only once. For the dose of 75 mg/kg: two dogs vomited twice. For the dose of 100 mg/kg: two dogs vomited three times, whereas one dog vomited 5 times.

The autofluorescence from the various sites showed little variation over the course of the study. ANOVA for autofluorescence ratios is shown in Table 1. There was no significant difference in the autofluorescence obtained from the dogs at various sites. The PpIX fluorescence attributable to the 5 mg/kg dose could be clearly quantified in one animal. For the other animals, the PpIX fluorescence due to the 5 mg/kg dose did not differ significantly from the autofluorescence. Peak fluorescence occurred between 2 and 6 hours, depending on the dose of ALA administered. The R/O ratio increased significantly for sites in the oral cavity after administration of ALA. For higher doses (>25 mg/kg), the R/O ratio was approximately 35 times higher than the autofluorescence ratio (Fig. 3). The R/O ratio was higher for higher doses of ALA, but the increase was not proportional to the dose. A typical graph of fluorescence kinetics is shown in Figure 3, com-

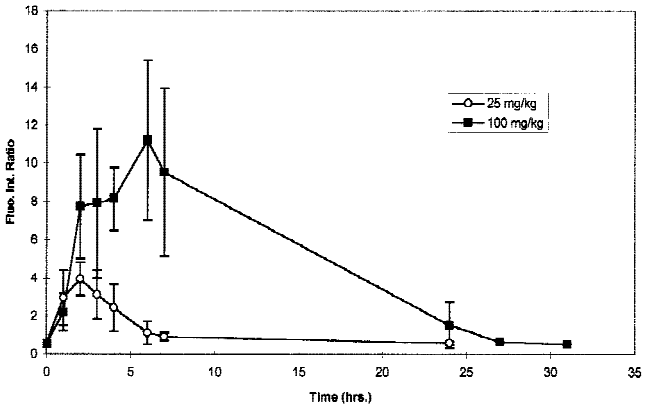

Fig. 3. Comparison of fluorescence kinetics from the gums after two doses of aminolevulinic acid (ALA): 25 and 100 mg/kg. For the higher dose, a shift to the right can be seen in the pharmacokinetics, indicating longer time to attain fluorescence peak.

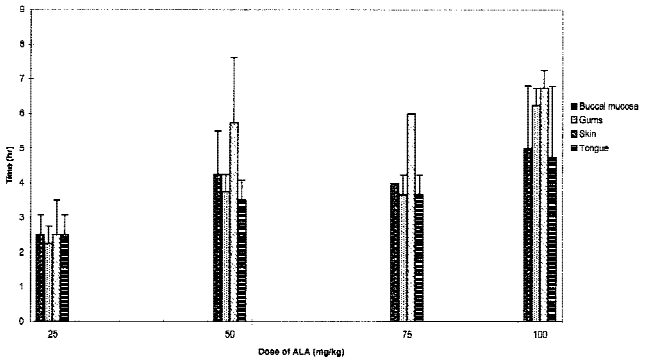

Fig. 4. Time taken to attain fluorescence peaks in various sites after various doses of ALA.

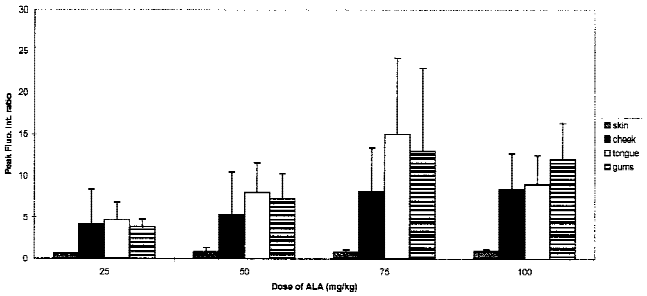

Fig. 5. Peak ALA-induced fluorescence at various sites due to various doses. Gums and the tongue showed highest peak fluorescence followed by the buccal mucosa and the skin.

paring doses of 25 and 100 mg/kg. As the graphs indicate, the fluorescence kinetics was dose dependent. For the higher dose of 100 mg/kg, peak fluorescence was seen later as signified by the shift to the right in fluorescence kinetics. For intermediate doses, the fluorescence ratios were not significantly different. The peak fluorescence ratios for a dose of 100 mg/kg were twice as high as those for the 25 mg/kg dose. For lower doses (<50 mg/kg), the PpIX fluorescence returned to the baseline (autofluorescence) levels in 24 hours. Higher doses of ALA showed the PpIX fluorescence returning to baseline in 27–31 hours. The fluorescence kinetics in Figure 3 show the fluorescence after the higher dose reaching baseline levels at a later time as opposed to baseline levels being reached in 24 hours for the 25 mg/kg dose. Figure 4 shows a graph for the typical time taken to attain peak fluorescence for various doses at various sites. For the dose of 25 mg/kg, peak fluorescence was attained 2–3 hours after ALA administration versus 3–4 hours for doses of 50 and 75 mg/kg. For the 100 mg/kg dose, peak fluorescence was observed 4–6 hours after ALA administration. The peak fluorescence obtained from the dogs at various sites for various doses is shown in Figure 5. The tongue and gums showed the highest peak fluorescence followed by buccal mucosa and skin. Peak fluorescence decreased for gums and tongue after a dose of 100 mg/kg. The drop in fluorescence could be due to the peak being missed for the 100 mg/kg dose at the sites. Mean separation tests (Student-Newman-Keuls procedure, $\alpha = 0.05$) were carried out to check for significant differences between fluorescence peaks, for doses of 75 and 100 mg/kg.

The peaks in plasma were attained earlier than at the sites in the oral cavity or skin. The plasma porphyrins peaked at 1 hour for lower doses and between 1 and 3 hours for higher doses. The typical kinetics for plasma porphyrins after two doses of ALA reached baseline values in 24 hours as shown in Figure 6. The peak value of plasma porphyrins after the dose of 100 mg/kg was twice that of the 25 mg/kg dose, which correlates well with the fluorescence data shown in Figure 3. A clear difference in kinetics can be seen for doses of 25 and 100 mg/kg (Fig. 6); however, kinetics for the doses of 50 and 75 mg/kg doses seemed similar. Mean separation tests (Student-Neuman-Keuls, $\alpha = 0.05$) were performed to check for significant differences in the plasma porphyrin kinetics due to doses of 50 and 75 mg/kg of ALA.

In the two dogs whose urine analysis was carried out after ALA administration, blood and protein were found in large quantities. The total porphyrins in the urine of the two dogs, 24 hours after ALA administration was estimated to be

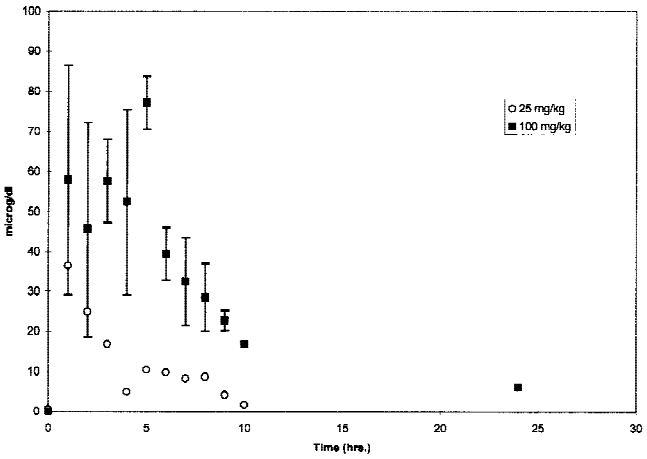

Fig. 6. Kinetics of plasma porphyrins after two doses of ALA, 25 and 100 mg/kg in dog 2. The plasma porphyrins peaked at 1 hour for lower doses and between 1 and 3 hours for higher doses of ALA.

2,570 and 2,580 nmol. The amount of ALA in the urine samples of the dogs was 2, and 8 mg, respectively. Predose urine was not collected.

The rate of synthesis of PpIX (k_1) and the rate of conversion of PpIX to heme products (k_2) were estimated by fitting the fluorescence data to the model (Eq. 1). The results are of particular interest when comparing pharmacokinetics caused by different doses and are illustrated in Tables 2 and 3. The rates were estimated by fitting the fluorescence data to the model (Eq. 1). The synthesis of PpIX is faster for the lowest dose compared with the highest dose, whereas the conversion to heme products for the highest dose is slower compared with the lowest dose. Two graphs of the model fit are shown in Figure 7a and b, along with fluorescence data, for doses of 25 and 100 mg/kg from the gums. To analyze further the rate of synthesis of PpIX and the rate of conversion of PpIX to heme products, mean separation procedures (Student-Neuman-Keuls, $\alpha = 0.05$) were carried out for various doses at each site in the oral cavity.

DISCUSSION

In the present study, the PpIX fluorescence kinetics seemed to be dose dependent, i.e., higher doses produced higher fluorescence peaks at later times in various sites. Under normal conditions, the demand for heme controls the rate of synthesis of heme and, therefore, the rate of synthesis of PpIX [7]. The presence of a large excess of ALA bypasses the ALA/heme feedback control. With the concentration of ALA no longer a limiting factor, the rate of synthesis of the next intermediate porphobilinogen is determined primarily by the maximum capacity of the enzyme, α-aminolevulinic acid dehydratase, that is responsible for converting ALA to porphobilinogen. What happens at each subsequent step may vary from tissue to tissue. The limitations imposed by the enzymatic reactions in the biosynthetic pathway could be responsible for slow attainment of PpIX peaks for higher doses of ALA as observed in Figures 3 and 4. The lower doses in comparison may not inhibit the enzymatic reactions as extensively, resulting in faster production and clearance of PpIX in the tissues. A decrease in peak fluorescence was observed (Fig. 5) for the tongue and the gums going from 75 to 100 mg/kg. However, mean separation procedures did not indicate a significant difference between the fluorescence peaks. The analysis of peak fluorescence data (Fig. 5) by using mean separation procedures suggests that the accumulation of PpIX in tissues reaches a plateau at higher doses of ALA.

Statistical analysis of the fluorescence data by using split-plot analysis indicated an interaction between sites and doses at all hours of data collection, barring the autofluorescence readings and the 24 hour reading, when the ALA-induced fluorescence has returned to baseline levels (Table 1). The resulting ANOVA can be interpreted (at $\alpha = 0.05$) to state that the effect of sites on fluorescence yield is not the same for all doses of ALA. Mean separation procedures (Student-Neuman-Keuls, $\alpha = 0.05$) were then carried out for each dose at every hour of data collection and also at each site for the same hours of data collection. The mean separation procedures indicated that the fluorescence ratios measured from the oral cavity were significantly different from those measured at the skin.

In a previous study on oral cancer in a hamster model, van der Breggen et al. [11] reported that the fluorescence ratio (R/O) after administration of ALA reached its peak value around 3.5 hours in premalignant facial skin, compared with 5 hours for normal skin for a dose of 40 mg/kg of ALA. They also showed that the fluorescence peak in transformed buccal mucosa was attained in 2–3 hours as opposed to 4 hours for normal buccal mucosa. It was found that the fluorescence ratio for transformed tissue was 2–4 times higher than that of normal tissue. Abels et al. [12] reported observing PpIX peaks in normal buccal mucosa (hamster) 4 hours after administration of 100 mg/

TABLE 2. Rates of Protoporphyrin IX Synthesis for Sites in the Oral Cavity, for Various Doses, as Obtained From the Compartmental Model

Sites/doses	Rate (1/hr)	25 mg/kg	50 mg/kg	75 mg/kg	100 mg/kg
Buccal mucosa	k_1	0.71 ± 0.06	0.31 ± 0.06	0.55 ± 0.12	0.34 ± 0.24
Gums	k_1	0.63 ± 0.35	0.57 ± 0.11	0.51 ± 0.08	0.14 ± 0.02
Tongue	k_1	0.58 ± 0.21	0.52 ± 0.12	0.49 ± 0.13	0.13 ± 0.04

TABLE 3. Rates of Conversion of Protoporphyrin IX to Heme Products for Sites in the Oral Cavity, for Various Doses, as Obtained From the Compartmental Model

Sites/doses	Rate (1/hr)	25 mg/kg	50 mg/kg	75 mg/kg	100 mg/kg
Buccal mucosa	k_2	0.65 ± 0.15	0.49 ± 0.12	0.57 ± 0.37	0.38 ± 0.15
Gums	k_2	1.42 ± 0.58	0.55 ± 0.08	0.53 ± 0.04	0.45 ± 0.31
Tongue	k_2	0.81 ± 0.29	0.55 ± 0.09	0.48 ± 0.17	0.50 ± 0.29

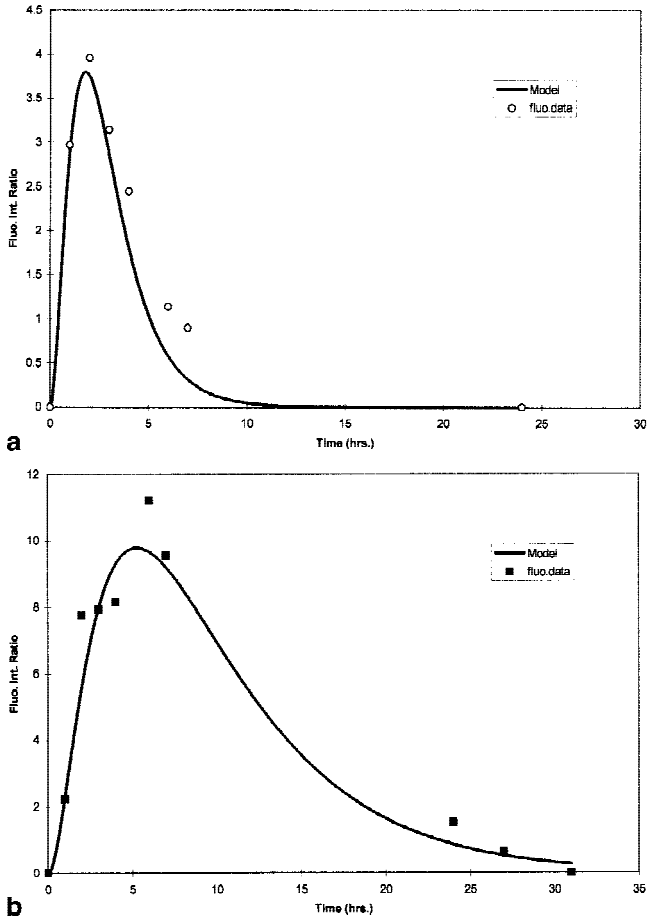

Fig. 7. The compartmental model fit and fluorescence data for **(a)** dose of 25 mg/kg of ALA at the gums, the rates are $k_1 = 0.63$, $k_2 = 1.42$, $k_x = 1.53$, all rates in units of hour^{-1}. **(b)** Dose of 100 mg/kg of ALA at the gums, the rates are $k_1 = 0.15$, $k_2 = 0.45$, $k_x = 1.37$, all rates in units of hour^{-1}.

kg of ALA. In our canine study, the PpIX fluorescence from the buccal mucosa attained peak values in 2–6 hours, depending on the dose. Comparatively, the PpIX fluorescence from the skin took longer to attain peak values for each dose (Fig. 4). The return of fluorescence to baseline values in 24 hours for lower doses (Fig. 3) is consistent with that reported by van der Breggen et al. [11] in the hamster cheek pouch model.

In our study, the sites in the oral cavity showed higher fluorescence peaks compared with the skin. Kennedy and Pottier [7] have stated that different cells and tissues have different capacities to synthesize PpIX and heme. The difference in the capacity to synthesize PpIX could lead to a corresponding variation in fluorescence from site to site. The comparatively higher vascularity of the gums and tongue could also be contributing to the synthesis of more PpIX at those sites, causing the fluorescence to be higher than that from the buccal mucosa and the skin. The buccal mucosa of some of the dogs used in this study showed extensive pigmentation (melanin). Melanin shows good absorption of light in the visible range [21]. The reabsorption of the emitted light at 636 nm would cause a decrease in the fluorescence emission detected by the probe. There is a significant difference in keratin composition of the skin versus the buccal mucosa [11]. Sterenborg et al. [22] demonstrated that keratin in the stratum corneum of human skin contributes significantly to the total fluorescence of the tissue, masking the ALA-induced fluorescence. As a result, the autofluorescence intensity (at 595 nm) of the skin is higher than that in the oral cavity. In our study, no significant differences were seen in the autofluorescence spectra obtained from various sites.

Another important factor to be considered is the variation in tissue optical properties from site to site. Wavelength-dependent absorption and scattering properties of tissue could affect the depth of the probing site and also the reabsorption of emitted light. The optical property of the

tissue could be influenced by the tissue vascularization. The use of a nondimensional fluorescence spectroscopic function (R/O) ensures that the measurements made are independent of such uncontrollable variations as distance variations and light source fluctuations. Although the R/O method minimizes the effect of tissue optical properties on measured fluorescence, one way to compensate for spatial variations in tissue optical properties would be to use the double-ratio technique suggested by Sterenborg et al. [23].

In our study, plasma porphyrin peaks were found earlier than in the oral cavity. Porphyrin concentrations in plasma were found to increase rapidly after administration of ALA, for all doses. Mean separation procedures did not indicate a significant difference in the plasma porphyrin kinetics attributable to doses of 50 and 75 mg/kg of ALA. The results we obtained are consistent with a previous study by Egger et al. [19]. Egger et al. observed that porphyrin concentrations in plasma increased rapidly after administration of an ALA dose of 100 mg/kg and then gradually decreased but were still markedly increased at 8 hours. It was also observed that the maximum plasma porphyrin concentrations after ALA administration were 50-fold greater than baseline values. Analysis of plasma porphyrins was done for a 10-hour study after ALA administration [19]. In comparison, our study examined plasma porphyrin kinetics over 24 hours. Our results indicate that the redistribution of PpIX by plasma is less influenced at the lowest dose than at the higher doses of ALA.

From Figure 6, plasma porphyrin levels at 1 hour after administration of ALA, for a dose of 100 mg/kg, is found to be 87 μg/dL (0.87 μg/ml). By using the theory developed by Jacques et al. [24], this value of PpIX is about 2% of the 42 μg/ml of PpIX in the idealized, uniform distribution of ALA. Tissue PpIX levels peak later than the peaks seen in plasma. The liver could be playing a major role in taking up most of the ALA and releasing PpIX into the blood. This mechanism lends credence to the role of plasma as a conduit for PpIX, mentioned earlier in this section. The tissue levels may be accumulating significant PpIX from the liver by means of the blood. The liver is particularly active in removing ALA from the blood stream and synthesizing PpIX [19]. A considerable amount of ALA is rapidly excreted in the urine and taken up by the organs with a high metabolic activity for ALA such as liver or kidney; hence, plasma levels will decrease rapidly [12]. For the highest dose of ALA used in this study (100 mg/kg), the liver is subjected to a large amount of ALA. Jacques et al. [24] reported that in the rat liver, levels of PpIX fluorescence were five times greater than an implanted tumor. This finding implies that the liver PpIX was fivefold above other soft-tissue levels. They measured the liver kinetics compared with the skin and tumor kinetics of PpIX fluorescence and reported the rate of PpIX build up in the liver was faster than the skin but comparable to that in other tissues. Egger et al. [19] have reported PpIX levels of about 0.2 μg/ml in skin, and 12 μg/ml in liver after administration of a dose of 100 mg/kg of ALA. Probably, oral tissues are approximately 2 μg/ml, much less than the expected PpIX levels for the idealized uniform and total conversion of ALA to PpIX.

Jacques et al. [24] reported that 200 mg/kg of ALA should yield 84 μg/ml of PpIX, assuming that ALA were to be distributed uniformly throughout the body, with complete conversion to PpIX. Hence, 100 mg/kg should yield 42 μg/ml of PpIX. The urine level of porphyrins at 24 hours for the two dogs that were given 100 mg/kg of ALA is 2,575 nmol (average). Assuming that it is all PpIX, the total amount of PpIX in the urine at 24 hours can be calculated as (2,575 nmol) (167.9 g/mol) = 0.43 mg. By using the theory developed by Jacques et al. [24], the total amount of PpIX expected to be synthesized is (42 μg/ml) (22 kg average weight of dog) (1,000 ml/kg) = 924 mg. Thus, very little of the PpIX is found in the urine, suggesting an alternate route of excretion of PpIX. The amount of ALA (average) in the urine of the two dogs was 5 mg. Given that the two dogs were administered 2,721 mg of ALA (average), only 0.2% of the original dose is seen in the 24-hour urine sample, indicating as previously mentioned, that the organs with high metabolic activity take up the ALA.

In our study, the results obtained from the compartmental model at first glance suggest a dose dependence of the kinetics of tissue PpIX levels. The rate of PpIX synthesis seems to decrease with increase in dose, whereas the conversion of PpIX to heme products is slower for higher doses compared with lower doses of ALA (Tables 2 and 3). Mean separation tests indicated that the rate of synthesis of PpIX in the gums and the tongue is not significantly different for doses $\leq$75 mg/kg. Above a threshold dose (possibly 75 mg/kg), the rate of PpIX synthesis seems to slow down (100 mg/kg; Table 2). In the buccal mucosa, the rate of

synthesis of PpIX is significantly different for the doses administered. The intermediate doses are not significantly different, whereas the extreme doses (25 and 100 mg/kg) are in a category of their own. The conversion of PpIX to heme products is significantly different for the 25 mg/kg dose compared with the higher doses. The higher doses do not show a significant difference in the conversion of PpIX to heme products. The rate of conversion of PpIX to heme seems to start changing more quickly at a lower threshold (25–50 mg/kg).

The pharmacokinetics of a drug are said to be nonlinear when one or more of the pharmacokinetic parameters vary with the dose, the concentration at a given time, or with time [25]. Nonlinearity occurs when one of the processes governing the behavior of a drug in the body varies with dose or time. The causes are numerous and could be related to absorption of the drug and the first-pass effect. This variation could occur because of the saturation of the hepatic enzyme system responsible for the first-pass effect, which has been alluded to earlier in this section. The causes of nonlinearity could also be related to distribution such as the saturation of plasma protein binding at high drug concentrations. Saturation of the transport system may also cause nonlinearity. Another cause of nonlinearity could be related to the metabolism of the drug caused by the enzyme system as the dose is increased. A progressive increase in dose will eventually lead to nonlinear pharmacokinetics. Therefore, in this sense, all drugs would be expected to show nonlinear pharmacokinetics, and this characteristic is of particular interest when it occurs at therapeutic doses.

From previous studies, it seems that administration of lower doses of ALA did not produce abnormal liver enzyme elevations [26]. Thus, a case can be made for administration of fractionated ALA doses. For example, four doses of 25 mg/kg of ALA could be administered at regular intervals, instead of one large dose of 100 mg/kg. This has particular relevance to PDT, for which use of high doses of ALA is common. The advantages of such a treatment in "installments" would be that the treatment procedure could be started earlier and continued at regular intervals as opposed to one consolidated, high dose. Also, hepatocellular toxicity may not be a concern. Administration of fractionated doses of ALA could also offer the benefit of fractionated light doses for PDT, thereby reducing the net light dose. Messmann et al. [27] investigated the enhancement of PDT with ALA-induced photosensitization in normal rat colon by fractionating the light dose. Their results seem to indicate that a short interruption in light radiation may dramatically reduce the net light dose required to achieve extensive necrosis.

For successful photodynamic diagnosis (PDD) and effective PDT with ALA-induced protoporphyrin IX, it is imperative to gain knowledge of the maximum fluorescence intensity after systemic administration of ALA. Hence, the study of time course of porphyrin accumulation and the effect of tissue type assumes significance. First-generation photosensitizers such as hematoporphyrin require that the animals be maintained in a darkened room or kennel for 2–3 weeks. In the present study, even with the highest dose of 100 mg/kg of ALA, fluorescence was back to baseline levels in 31 hours; thus, the use of ALA seems preferable for diagnostic and therapeutic purposes. The results presented in this study have implications for optical diagnosis of oral cancer as well as the safe use of high doses of ALA for PDT. More investigation with doses of 5 and 25 mg/kg on animals with cancer is required.

CONCLUSIONS

In this study, we conducted in vivo fluorescence spectroscopic detection in dogs to investigate the effect of drug dose and tissue type on ALA-induced, protoporphyrin IX fluorescence. The ALA doses used in the study were well tolerated by the animals. The study showed that the timing of the fluorescence peak was dose dependent at all sites. It was also observed that the tongue and the gums showed the highest peak fluorescence values, followed by the buccal mucosa and the skin. The dose dependence of the kinetics of peak tissue is consistent with the liver absorbing most of the ALA and redistributing the PpIX to the other tissues, especially at higher doses. The high amount of plasma PpIX, which forms very quickly, is comparable to the probable concentration of PpIX in oral tissues. Yet, tissue levels of PpIX reach a peak later than plasma, whereas plasma PpIX levels continue to fall after the initial rapid rise.

The oral cavity is easily accessed with a fiber optic probe; hence, it is a suitable site for fluorescence diagnostics. Fluorescence ratio measurements made after administration of ALA could assist in the differentiation of neoplastic tissue from normal tissue, especially during the early stages of neoplasia. The present study suggests

that low doses of ALA seem to be safe for diagnostic purposes, although more studies are needed on ALA-induced hepatotoxicity in dogs for higher doses with regard to PDT.

ACKNOWLEDGMENT

Sincere thanks are extended to Ms. Eunsug Park of the Department of Statistics, Texas A&M University, for her suggestions on the statistical analysis.

REFERENCES

1. Ingrams DR, Dhingra JK, Roy K, Perrault DF, Bottrill ID, Rebeiz EE, Kabani S, Pankratov MM, Manoharan R, Itzkan I, Shapshay SM, Feld MS. Autofluorescence characteristics of oral mucosa. Head Neck 1997;19:27–32.
2. Yang Y, Katz A, Celmer EJ, Szczepaniak MZ, Alfano RR. Fundamental differences of excitation spectrum between malignant and benign breast tissues. Photochem Photobiol 1997;66:518–522.
3. Hayata Y, Kato H. Photodynamic therapy in the treatment of early cancer. In: Dougherty TJ, Henderson BW, editors. Photodynamic therapy: basic principles and clinical application. New York: Marcel Dekker; 1992. p 269–278.
4. Kelley EE, Domann FE, Buettner GR, Oberley LW, Burns CP. Increased efficacy of in vitro photofrin photosensitization of human squamous cell carcinoma by iron and ascorbate. Photochem Photobiol B Biol 1997;40:273–277.
5. Fan KFM, Hopper C, Speight PM, Buonaccorsi GA, Bown SG. Photodynamic therapy using MTHPC for malignant disease in the oral cavity. Int J Cancer 1997;73:25–32.
6. Orenstein A, Kostenich G, Roitman L, Schectman Y, Kopolovic Y, Ehrenberg B, Malik Z. A comparative study of tissue distribution and photodynamic therapy selectivity of chlorin e6, photofrin II and ALA-induced protoporphyrin IX in a colon carcinoma model. Br J Cancer 1996;73: 937–944.
7. Kennedy JC, Pottier RH. Endogenous protoporphyrin IX, a clinically useful photosensitizer for photodynamic therapy. Photochem Photobiol 1992;14:275–292.
8. Berns BW, Dahlman A, Johnson FM, Burns R, Sperling D, Guiltinan M, Siemens A, Walter R, Wright W, Hammer-Wilson M, Wile A. In vitro cellular effects of hematoporphyrin derivative. Cancer Res 1982;42:2325–2329.
9. Shulok JR, Wade MH, Lin CW. Subcellular localization of hematoporphyrin derivative in bladder tumor cells in culture. Photochem Photobiol 1990;51:451–457.
10. Wilson BC, Olivo M, Singh G. Subcellular localization of photofrin and aminolevulinic acid and photodynamic cross-resistance in vitro in radiation induced fibrosarcoma cells sensitive or resistant to photofrin-mediated photodynamic therapy. Photochem Photobiol 1997;65: 166–176.
11. van der Breggen EWJ, Rem AI, Christian MM, Yang CJ, Calhoun KH, Sterenborg HJCM, Motamedi M. Spectroscopic detection of oral and skin tissue transformation in a model for squamous cell carcinoma: autofluorescence vs systemic ALA-induced fluorescence. [Accepted for publication by IEEE J of Selected Topics in Quantum Electronics].
12. Abels C, Heil P, Dellian M, Kuhnle GEH, Baumgartner R, Goetz AE. In vivo kinetics and spectra of 5-aminolevulinic acid-induced fluorescence in an amelanotic melanoma of the hamster. Br J Cancer 1994;70:826–833.
13. Grant WE, Hopper C, MacRobert AJ, Speight PM, Bown SG. Photodynamic therapy of oral cancer: photosensitisation with systemic aminolevulinic acid. Lancet 1993; 342:1471–148.
14. Leunig A, Rick K, Strepp H, Gutmann R, Goetz AE, Baumgartner R, Feyh J. Fluorescence imaging and spectroscopy of 5-aminolevulinic acid induced protoporphyrin IX for the detection of neoplastic lesions in the oral cavity. Am J Surg 1996;172:674–677.
15. Fan KF, Hopper C, Speight PM, Buonaccorsi G, MacRobert AJ, Bown SG. Photodynamic therapy using 5-aminolevulinic acid for premalignant and malignant lesions of the oral cavity. Cancer 1996;78:1374–1383.
16. Webber J, Kessel D, Fromm D. Side effects and photosensitization of human tissues after aminolevulinic acid. J Surg Res 1997;68:31–37.
17. Profio AE, Dioron DR, Sarnaik J. Fluorometer for endoscopic diagnosis of tumors. Med Phys 1984;11:516–520.
18. Schwartz S, Edmonson P, Stephenson B, Sarkar D, Freyholtz H. Direct spectrofluorometric determination of porphyrin in diluted urine. Ann Clin Res 1976;8:156–161.
19. Egger NG, Motamedi M, Pow-Sang M, Orihuela E, Andersen KE. Accumulation of porphyrins in plasma and tissues of dogs after delta-aminolevulinic acid administration: implications for photodynamic therapy. Pharmacology 1996;52:362–370.
20. Vaidyanathan V, Rastegar S, Fossum TW, Flores P, van der Breggen EWJ, Egger NG, Jacques SL, Motamedi M. In vivo kinetics of ALA-induced fluorescence in the canine oral cavity: influence of drug dose and tissue type. Proc SPIE 1997;975:222–226.
21. Britton G. The biochemistry of natural pigments. New York: Cambridge University Press; 1983.
22. Sterenborg HJCM, Motamedi M, Wagner RF, Duvic M, Thomsen S, Jacques SL. In-vivo fluorescence spectroscopy and imaging of human skin tumors. Lasers Med Sci 1994;9:191–201.
23. Sterenborg HJCM, Saarnak AE, Frank R, Motamedi M. Evaluation of spectral correction techniques for fluorescence measurements on pigmented lesions in vivo. Photochem Photobiol B Biol 1996;35:159–165.
24. Jacques SL, Rodriguez T, Schwartz J. Kinetics of ALA-induced protoporphyrin IX accumulation in the liver, skin, and tumor of a rat model. In: Dougherty T, editor. Optical methods for tumor treatment and detection: mechanisms and techniques in photodynamic therapy IV. SPIE Proceedings, San Jose, CA, 1995;2392:1–8.
25. Labaune J-P. Handbook of pharmacokinetics, toxicity assessment of chemicals, Chichester: Ellis Horwood Press; 1989.
26. Fossum TW, Vaidyanathan V, Rastegar S, Flores P, Edwards J, Motamedi M. Clinical Evaluation of 5-aminolevulinic acid administration in normal dogs. ASLMS Abstracts 1997;236:52.
27. Messmann H, Mlkvy P, Buonaccorsi G, Davies CL, MacRobert AJ, Bown SG. Enhancement of photodynamic therapy with 5-aminolevulinic acid-induced porphyrin photosensitization in normal rat colon by threshold and light fractionation studies. Br J Cancer 1995;72:589–594.